



## Characterization of PI:PCBM organic nonvolatile resistive memory devices under thermal stress



Youngrok Kim<sup>a</sup>, Daekyoung Yoo<sup>a</sup>, Jingon Jang<sup>a</sup>, Younggul Song<sup>a</sup>, Hyunhak Jeong<sup>a</sup>,  
Kyungjune Cho<sup>a</sup>, Wang-Taek Hwang<sup>a</sup>, Woocheol Lee<sup>a</sup>, Tae-Wook Kim<sup>b, \*\*</sup>, Takhee Lee<sup>a, \*</sup>

<sup>a</sup> Department of Physics and Astronomy, Institute of Applied Physics, Seoul National University, Seoul, 08826, South Korea

<sup>b</sup> Soft Innovative Materials Research Center, Institute of Advanced Composite Materials, Korea Institute of Science and Technology, Joellabuk-do, 55324, South Korea

### ARTICLE INFO

#### Article history:

Received 8 January 2016

Received in revised form

5 March 2016

Accepted 9 March 2016

Available online 15 March 2016

#### Keywords:

Organic memory

Nonvolatile memory

PI:PCBM

Thermal stress

Robustness

### ABSTRACT

In this study, we fabricated nonvolatile organic memory devices using a mixture of polyimide (PI) and 6-phenyl-C61 butyric acid methyl ester (PCBM) (denoted as PI:PCBM) as an active memory material with Al/PI:PCBM/Al structure. Upon increasing the temperature from room temperature to 470 K, we demonstrated the good nonvolatile memory properties of our devices in terms of the distribution of ON and OFF state currents, the threshold voltage from OFF state to ON state transition, the retention, and the endurance. Our organic memory devices exhibited an excellent ON/OFF ratio ( $I_{ON}/I_{OFF} > 10^3$ ) through more than 200 ON/OFF switching cycles and maintained ON/OFF states for longer than  $10^4$  s without showing any serious degradation under measurement temperatures up to 470 K. We also confirmed the structural robustness under thermal stress through transmission electron microscopy cross-sectional images of the active layer after a retention test at 470 K for  $10^4$  s. This study demonstrates that the operation of PI:PCBM organic memory devices could be controlled at high temperatures and that the structure of our memory devices was maintained during thermal stress. These results may enable the use of nonvolatile organic memory devices in high temperature environments.

© 2016 Elsevier B.V. All rights reserved.

## 1. Introduction

Organic electronic devices, including organic light-emitting diodes, solar cells, sensors, field effect transistors, and memory, have been widely investigated due to their merits, such as low cost and large-area fabrication, solution processes, and mechanical flexibility [1–7]. Organic resistive memory is among the promising future data storage devices for next-generation flexible electronic applications [8–10]. Diverse approaches such as the development of new materials, the design of architectures and the integration of memory cells have been attempted [11,12]. In particular, material research is one of the most important aspects because the performance of a memory device mainly depends on the properties of the active components [13–15].

Since Ouyang et al. reported programmable electrical bistability in a device with a polystyrene film containing gold nanoparticles,

there have been intensive studies on resistive switching from the mixture of an organic material and nanoparticles [16,17]. As a representative organic resistive material system, resistive switching has been observed in a certain ratio between the organic matrix and the nanoparticle filler [8,13,16,17]. The device performance depends on the total amount of the filler or the degree of dispersion in the organic matrix under mild environment. However, it has been reported that organic matrix materials such as polystyrene and poly(methyl methacrylate) (PMMA) exhibit poor resistance under thermal stress, which can cause organic material decomposition, bond breakage between atoms, phase transition, and transformation of the material's molecular structure configuration [18–21]. To use organic materials as an active component in practical memory application, it is necessary to verify both the robustness of the materials and the reliability of the devices due to their relatively poor performance compared to silicon-based memory devices. Recently, a polyimide-based polymer has been considered as a potential candidate matrix material for organic resistive memory due to its stable electrical insulating property and its excellent robustness under mechanical, chemical, and thermal

\* Corresponding author.

\*\* Corresponding author.

E-mail addresses: [twkim@kist.re.kr](mailto:twkim@kist.re.kr) (T.-W. Kim), [tlee@snu.ac.kr](mailto:tlee@snu.ac.kr) (T. Lee).

stresses [22,23]. The mixture of polyimide (PI) and 6-phenyl-C61 butyric acid methyl ester (PCBM) (denoted as PI:PCBM) has been employed to demonstrate various organic resistive memory applications, such as ones involving transistors or diodes to prevent cross-talk leakage problems, 3-dimensional vertical stacking, and micro-scale integration [24–28]. Although the PI:PCBM system has shown its potential as an active layer of memory devices, there have been few reliability studies of PI:PCBM memory devices under thermal stress. Generally, device reliability is considered as the ability to maintain the required electrical function during a specified period. The evaluation of reliability is an investigation of the stability of the electrical function over time or switching cycles. For inorganic materials-based memory devices, the obvious degradation of electrical functionality has been reported under high-temperature conditions, for example, malfunctions in resistive switching or reductions in retention time [29–32]. Therefore, a systematic and thorough reliability study on organic resistive memory under high-temperature conditions is necessary.

In this study, we evaluated the electrical stability of PI:PCBM organic resistive memory from room temperature to 470 K. The memory properties were characterized in terms of resistive switching characteristics, parameter uniformity, and device robustness at elevated temperatures. Parameter uniformity was investigated by means of plotting threshold voltages and criteria of the ON and OFF states of each memory cell under various temperature conditions. We also confirmed parameter uniformity by verifying 32 cells of memory for each temperature and measured both retention and sweep endurance. Finally, we verified the structural robustness before and after testing the retention characteristics at 470 K using transmission electron microscopy and atomic force microscopy.

## 2. Experimental section

### 2.1. Material preparation

Fig. 1(a) shows the molecular structures of the active memory material, PI:PCBM. To prepare the active layer, we prepared a mixture of 3 ml of biphenyltetracarboxylic acid dianhydride *p*-phenylene diamine (BPDA-PPD) solution (10 wt% in *N*-methyl-2-pyrrolidone (NMP), purchased from Sigma-Aldrich) as a PI block precursor and 9 ml of NMP to optimize the concentration of the solution. Then, we prepared 0.5 wt% 6-phenyl-C61 butyric acid methyl ester (PCBM, Sigma-Aldrich) solution in NMP. Next, BPDA-PPD and PCBM solutions were mixed at a volume ratio of 1:0.3. Subsequently, the PI:PCBM solution was sonicated for 10 min to improve the dispersion of PCBM in the BPDA-PPD solution. Finally, the prepared solution was filtered through a 0.45- $\mu\text{m}$  PTFE syringe filter to improve the surface uniformity of the active layer.

### 2.2. Fabrication process

Glass substrates were carefully cleaned using acetone, isopropanol, and de-ionized water for 10 min per cleaning solvent under sonication in an ultrasonic bath. The substrates were then placed in a vacuum oven at 100 °C for 2 h to remove residual solvents from the 1.5 × 1.5 cm<sup>2</sup> glass substrates. Next, 30 nm-thick bottom Al electrodes were deposited through a shadow mask on the substrates by thermal evaporation with an evaporation rate of 0.5 Å/s at a pressure of 10<sup>-6</sup> torr. The line width of the bottom Al electrodes was 100  $\mu\text{m}$ . Next, the bottom Al electrodes and substrates were treated with UV-ozone to improve the surface uniformity and enhance the memory properties [9,33,34]. The prepared PI:PCBM active layer solution was spin-coated on the substrates at 500 rpm for 5 s and then at 2000 rpm for 35 s. Then,

the film was annealed on a hot plate at 120 °C for 5 min and mopped with a cotton stick soaked in methanol to expose the bottom electrodes. The memory devices were hard baked on the hot plate at 300 °C for 30 min for the block-polymerization of PI. Finally, the top Al electrodes were deposited by the same procedure as for the bottom electrodes. The schematic of the fabricated device is shown in Fig. 1(b). The memory cell size was defined as 100 × 100  $\mu\text{m}^2$ . A more detailed description of the device fabrication processes is provided in the supplementary material (see Fig. S1 in supplementary material). The resulting thicknesses of the PI:PCBM layer and Al electrodes were found to be approximately 25 nm and 30 nm, respectively, by cross-sectional transmission electron microscopy (TEM, JEOL JEM-2100F) (see right image of Fig. 1(c)). The energy dispersive X-ray spectroscopy (EDS) data are provided as lines in Fig. 1(c) over a TEM cross sectional image. According to the EDS data, Al was not found in the organic PI:PCBM active layer, which supports a distinct separation between the organic active layer and the Al electrodes. Because Al penetration into the organic layer would create a metal filamentary path between the top and bottom electrodes and create short circuits in the memory devices, confirmation of the absence of Al in the memory active layer is important to demonstrate the effectiveness of the organic memory layer, indicating that the resistive switching characteristics of our memory devices originate from the organic active layer [15,35].

### 2.3. Electrical measurement

The electrical measurements of the PI:PCBM memory devices were performed using a semiconductor analyzer system (Model 4200-SCS, Keithley Inc.) at elevated high temperatures range from room temperature to 470 K under pressure of approximately 10<sup>-2</sup> mbar in a vacuum probe station with a temperature controller (Model ST-500, Janis Research Co.). To verify the structural robustness of the PI:PCBM active layer under thermal stress, we investigated PI:PCBM memory devices with cross-sectional TEM images and atomic force microscopy (AFM, Park Systems NX 10) images before and after the retention measurement at 470 K for 10<sup>4</sup> s.

## 3. Results and discussion

### 3.1. Resistive switching characteristics at elevated temperatures

Fig. 2(a) shows the current-voltage (I-V) curves of a selected memory device measured under different temperature conditions (300, 358, 420, and 470 K). The bottom electrodes were grounded, and the external voltage was applied to the top electrode. The typical resistive switching characteristics of PI:PCBM system have often shown a unipolar type with reversible switching properties at the same bias polarity [34,36]. The initial state of the memory devices remained in a high-resistive state (HRS, OFF state). To set the memory device from HRS to a low-resistive state (LRS, ON state), a voltage sweep was performed from 0 to 5 V and then back from 5 to 0 V to verify the resistance state of the programmed memory device. The resistive switching was clearly observed at approximately 3 V, showing an abrupt current jump of 3 orders of magnitude. The memory device showed negative differential resistance (NDR) between 5 and 8 V, implying that the resistance state changes from LRS to HRS. In particular, there were negligible differences in both the NDR ranges and the current levels under different temperature conditions (Fig. 2(a)). The devices exhibited a high ON/OFF ratio (>10<sup>4</sup>) for all temperature conditions, as shown in Fig. 2(b). These results indicate that our memory devices operated up to 470 K without loss of memory properties, maintaining their pristine

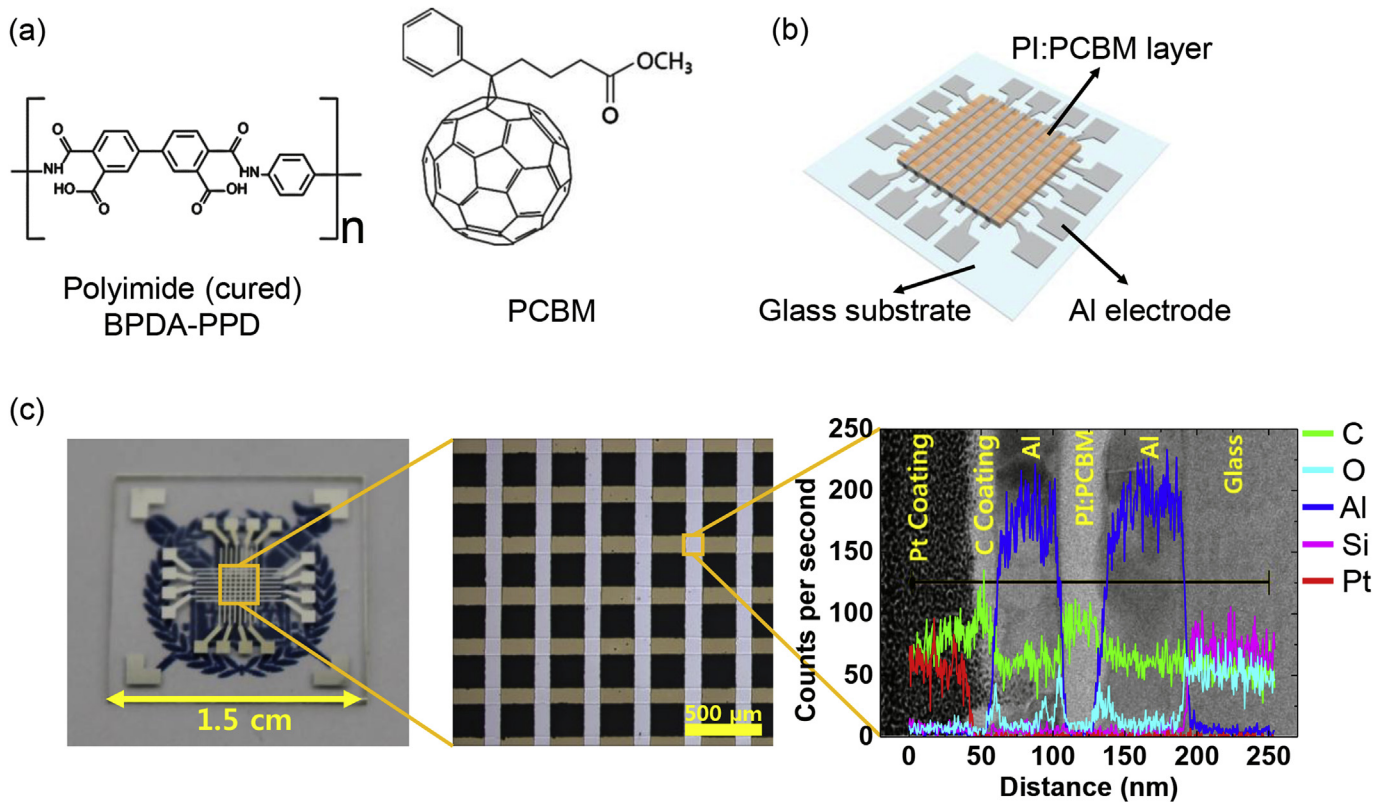


**Fig. 1.** (a) Chemical structure of cured PI and PCBM used as the active memory layer. (b) Schematic image of organic memory devices. (c) Optical image and TEM cross-sectional image of the fabricated organic memory devices. PI:PCBM layer is approximately 25 nm thick and well distinguished from both Al electrodes. EDS data are represented as lines over the TEM cross sectional image. Both the TEM cross sectional image and the EDS data showed clear separation of the organic active layer and Al electrodes.

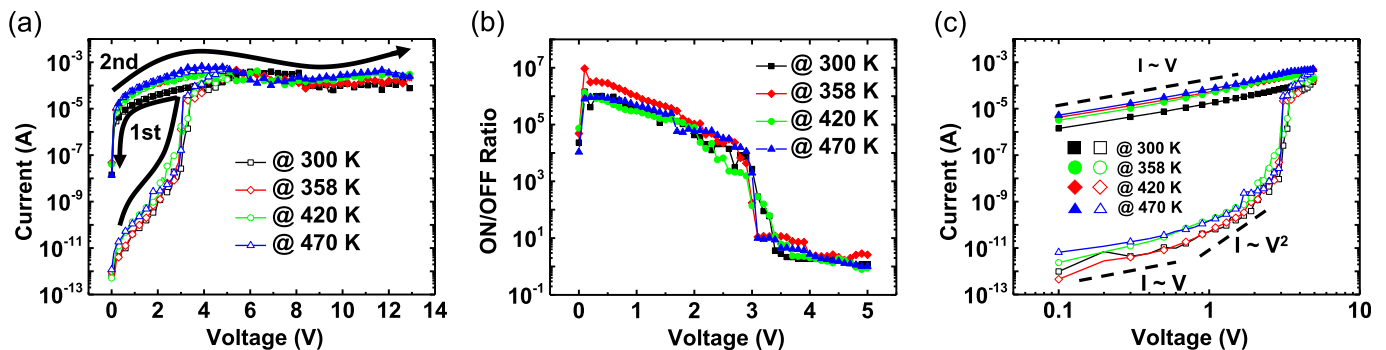


**Fig. 2.** (a) Characteristic I-V curves of organic memory devices with temperature elevation at the same cross point of bottom and top electrodes. I-V curves represent data at 300 K (black), 358 K (red), 420 K (green), and 470 K (blue). (b) ON/OFF current ratio of the memory cells versus applied bias for temperature variation from (a). (c) Logarithmic scales of I-V curves in 0–5 V region for each temperature. (For interpretation of the references to colour in this figure legend, the reader is referred to the web version of this article).

resistive switching characteristics as shown at room temperature.

In our previous study on the temperature dependence of the ON/OFF ratio of organic memory devices, memory devices with various types of polyfluorene-derivatives showed considerable degradation of the ON/OFF ratio under elevated temperature conditions [37]. We observed that both space charge-limited current conduction and filamentary conditions with metal ions in the polymer layer contributed to the resistive switching behavior, and the ON/OFF ratios began to considerably decrease at high temperatures due to the movement of metal ions in the polymer layer [37]. Therefore, it seems that the thermal robustness of the active layer may affect the reliability of the device operation. As shown in Fig. 2(a), we clearly observed temperature-independent I-V

characteristics. From the logarithmic scale plot of both current and voltage (Fig. 2(c)), for the OFF curve (open symbols), we found that the current flow shows almost linear like behavior ( $I \sim V$ ) at the low voltage regime under 1 V and nearly quadratic variation ( $I \sim V^2$ ) from 1 to 2 V for all temperatures. This is a typical space charge-limited current (SCLC) flow, exhibiting the trap-free-like region in which the trap site cannot be charged and the threshold voltage region as the trap charging region of SCLC [38,39]. For the ON curve (filled symbols), the I-V curves showed an almost linear dependence of current on voltage, and the charge flowed along the conduction path made by the trap sites, which are completely filled [15]. The current flows showed ohmic conduction behavior in the ON state up to 470 K. The PCBM in the PI layer assist the current

flows in both the ON and OFF states of the memory device. Moreover, because the polyimide matrix maintains its superior chemical, mechanical, and thermal stability, and the PCBM s are completely crosslinked in the matrix layer after the imidization process [22,23,40,41], our PI:PCBM system is expected to be a good candidate for reliable organic resistive switching memory devices.

### 3.2. Device parameter uniformity at elevated temperatures

Fig. 3 illustrates the statistical summary of the device-to-device uniformity and threshold voltages of the characterized memory devices. To verify the device yield, we measured the I-V sweep characteristics of each device. Eighty-three of the selected 88 cells operated at room temperature, and the estimated device yield was 94.3%. We characterized all of them under various temperature conditions. Fig. 3(a) illustrates the cumulative probability of the ON state current and OFF state currents for all of the memory devices operated under various temperature conditions (read voltage 0.3 V). The distributions of the ON current levels (filled symbols) were within two orders of magnitude. Although the OFF current levels (open symbols) showed a somewhat wider distribution than the ON current levels, the ON and OFF currents were well separated, showing a gap of more than two orders of magnitude at all the measured temperature conditions (from room temperature to 470 K).

Fig. 3(b) shows the statistical data on the threshold voltage ( $V_{th}$ ) at each temperature. By using Gaussian fitting analysis of each threshold voltage distribution, the standard deviation of the threshold voltages were found to be within 0.3 V for all temperatures, and all the mean values were near 3.3 V (see Fig. S2 in supplementary material for detailed results of Gaussian fitting and mean value distribution). Although the threshold voltage seems to slightly decrease with increasing temperature, there was no significant difference in the threshold voltage distributions of our organic resistive memory devices (see Fig. S3 in supplementary material for all I-V curves for each temperature).

### 3.3. Stability under thermal stress

To verify the memory storage durability and device stability, repeated I-V sweep endurance and retention tests were performed on our memory devices. Fig. 4(a) and (c) show the repeated DC sweep endurance tests to investigate device switching durability at 300 K and 470 K. The memory cell was turned ON and OFF by applying a DC double sweep from 0 to 4 V and a single sweep from

0 to 11 V, respectively. These turn-on and turn-off processes were repeatedly performed at each temperature without any interval time between on and off events. We read current values at 0.3 V for each ON and OFF state. Although there were some variations in the ON and OFF currents, our memory devices held a high ON/OFF ratio of over  $10^3$  during 200 repeated switching cycles for all temperatures. In addition, we measured the current level of the ON and OFF states for  $10^4$  s with a measurement interval of 10 s at a read voltage of 0.3 V to confirm that our memory device maintained its nonvolatile property for a sufficiently long time. Fig. 4(b) and (d) show the results of the retention tests for 300 K and 470 K. The current level ratios of the ON and OFF states were well maintained for more than  $10^4$  s without any serious degradation for both states (endurance and retention test results at 358 K and 420 K are presented in Fig. S4 in the supplementary material). After the retention test at 470 K, we performed DC sweeps on the memory devices again, and the two curves showed very similar features (see Fig. S5 in the supplementary material for the comparison of the two I-V curves).

It is well known that most electronic device failures are caused by thermal related issues. Therefore, to evaluate the electrical stability of our device under thermal stress, we analyzed the current variation of the ON and OFF states over time. In contrast to the repeated sweep endurance test, we performed a DC sweep during 1 h with a time interval of approximately 300 s at both 300 K and 470 K. We monitored the shape of the I-V curves, threshold voltage and ON/OFF ratios. We found that the ON and OFF state current levels of the memory devices for each sweep did not change significantly at 300 K and 470 K, as shown in Fig. 5 (results at 358 K and 420 K are presented in Fig. S6 in the supplementary material).

We have confirmed that our organic memory devices retain functionality as memory devices under thermal stress. It is also important to verify if there is any structural deformation or change in the atomic composition of the layers of our memory devices before and after thermal stress. We compared TEM cross sectional images and AFM images of memory devices before and after annealing through a retention test at 470 K for  $10^4$  s. Fig. 6(a) displays the TEM cross-sectional image and the EDS data after annealing. We did not identify any significant differences between the images in Figs. 1(c) and 6(a). The thickness of the PI:PCBM layers was measured to be 25 nm by cross sectional TEM analysis. The EDS data also showed that the elements of each part of the memory device did not change after the annealing test, implying that there was no formation of filamentary paths of aluminum and no deformation of the device structure (detailed EDS data are

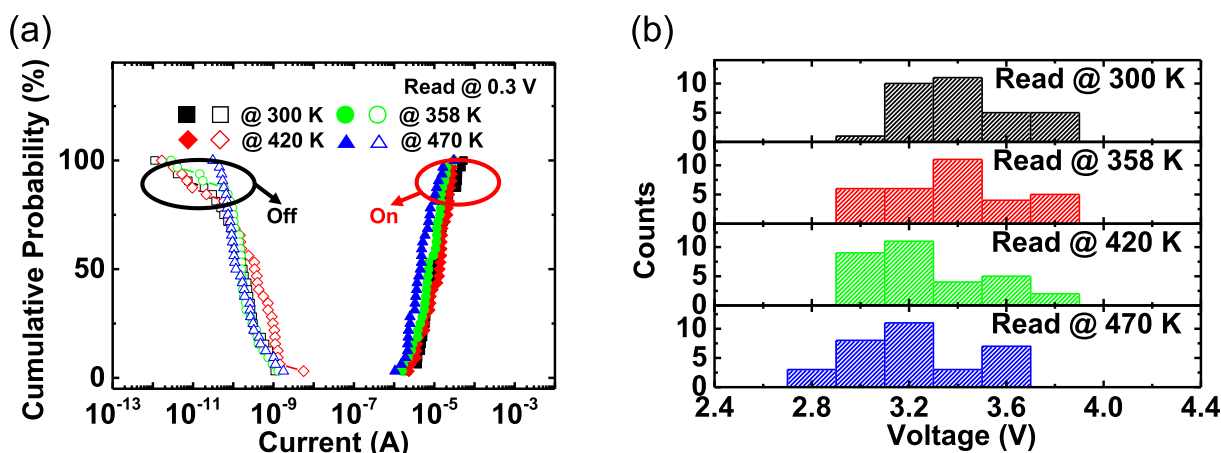


Fig. 3. (a) Cumulative probability of ON and OFF currents of 32 cells for each temperature. (b) Threshold voltage distribution at each temperature.

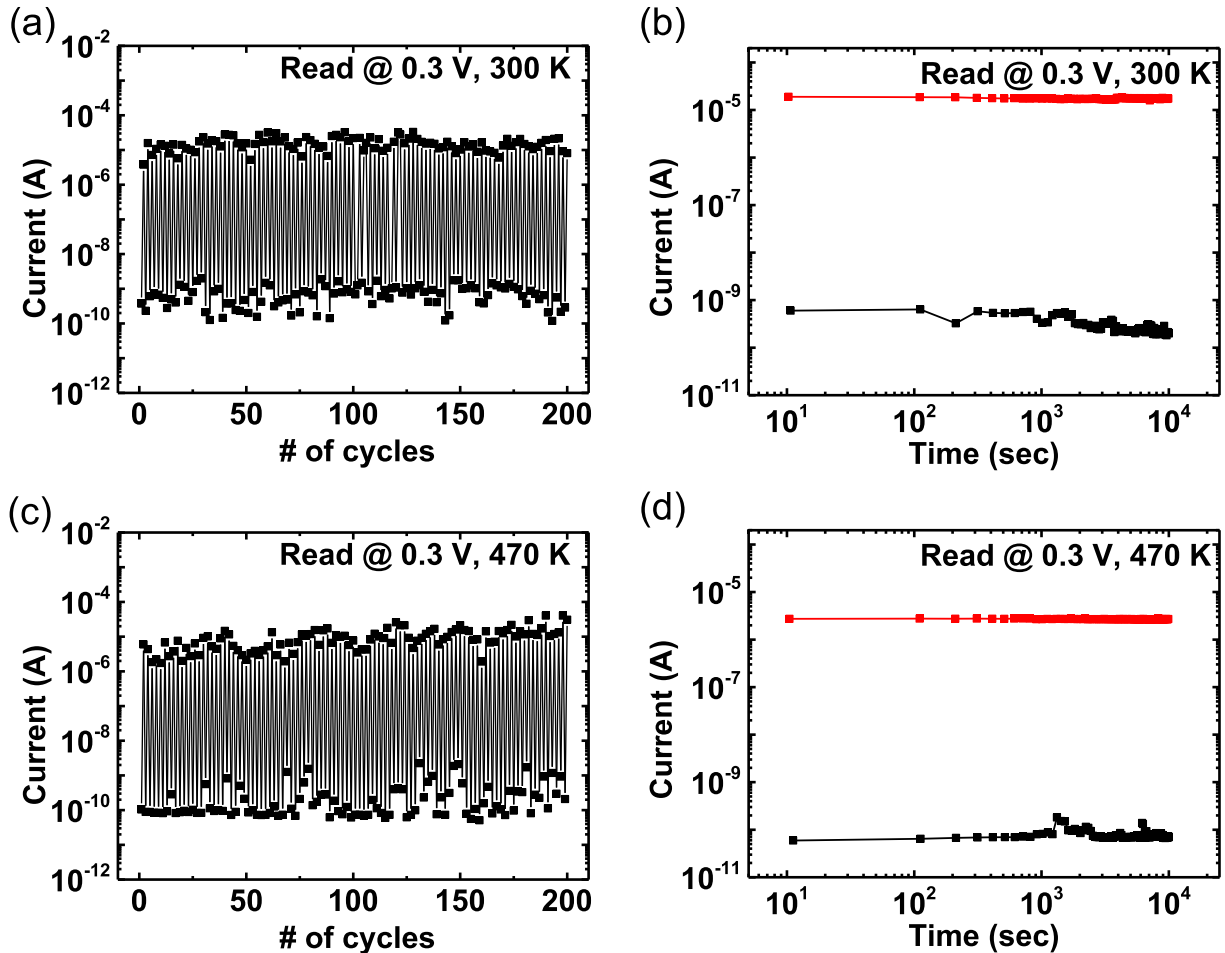


Fig. 4. (a) DC sweep endurance test and (b) retention time test results at 300 K. (c) DC sweep endurance test and (d) retention time test results at 470 K.

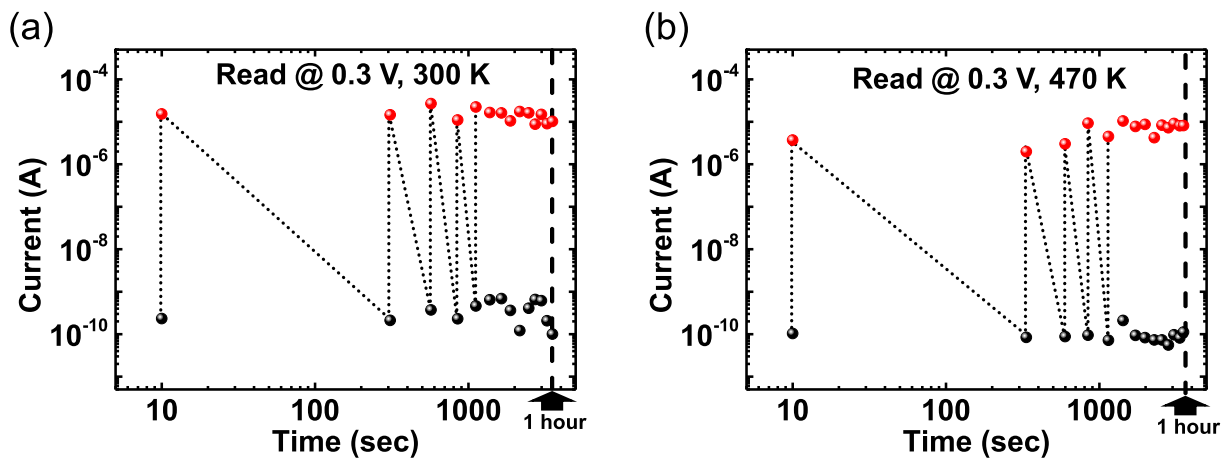


Fig. 5. Time versus current level data at (a) 300 K and (b) 470 K. The time interval between the data points is approximately 300 s.

provided in Fig. S7 in the supplementary material).

We also performed further analysis on the exposed PI:PCBM surface on the device substrate. Fig. 6(b) shows AFM images of the PI:PCBM layer surfaces before and after annealing. AFM images of the pristine PI:PCBM sample exhibited relatively rough surfaces with a few pinhole-like structures with a diameter of less than 200 nm and depth of less than 10 nm (Fig. 6(b)). These porous

structures seem to have been created by the evaporation of solvent (NMP) during the baking processes [40]. Considering the depth, the porous structure on the PI:PCBM layer did not contribute to conformation of an aluminum filamentary path between the top and bottom electrodes, which would generate short circuits instead of electrical memory behavior. We did not observe any significant difference in the surfaces from AFM images, implying structural

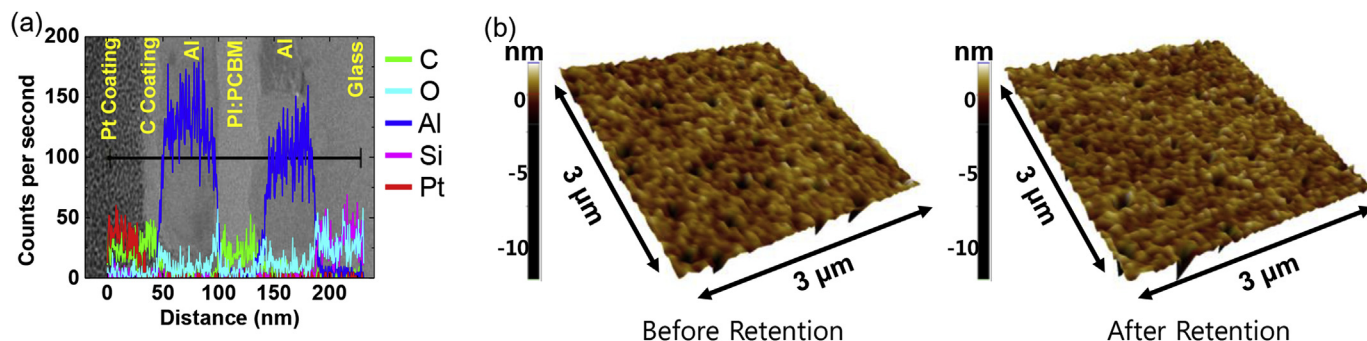


Fig. 6. (a) TEM cross-sectional image and EDS data after annealing by retention at 470 K for  $10^4$  s (b) AFM surface image of exposed PI:PCBM active layer before and after annealing.

robustness of the PI:PCBM active memory layer under thermal stress. The electrical and structural thermal robustness are presumed to be due to the thermal stability of polyimide, the matrix of the PI:PCBM organic memory layer, because the transition temperature of polyimide is generally higher than 400 °C.

Both structural robustness of organic layer and thermal stability of polyimide imply that the composite structures of PI:PCBM are maintained up to 470 K. So, charge traps caused by PI:PCBM composite structure are still maintained at high temperatures. As previous study for PI:PCBM conduction mechanism, charge trap sites constitute conduction path when they are filled, and the depth of the trap sites is more than 2 eV [15]. Therefore, the depth of charge trap sites can be maintained over 2 eV up to 470 K by structural robustness of organic layer. On the other hand, the thermal energy of the trapped charges increases as temperature rises. From room temperature to 470 K, thermal energy of the trapped charge changes from 25.9 to 40.5 meV. So, in spite of temperature increase, the charge in trap sites still overcomes similar energy barrier to free. Therefore, large depth of trap sites compared with thermal energy can result in the stable memory characteristics at high temperatures.

#### 4. Conclusions

In this study, we verified the thermal robustness of PI:PCBM unipolar organic resistive memory devices through confirmation of their electrical and structural robustness under elevated temperature conditions. PI:PCBM organic memory devices exhibited stable resistive switching performance such as similar current levels, steady ON/OFF ratio, and unchanged conductive features. From the retention, endurance cycles, and thermal stress tests, we found that stable resistive switching of the PI:PCBM memory devices was persistent at high temperature. Additionally, we verified the structural robustness of our PI:PCBM organic memory under thermal stress by cross-sectional TEM, EDS, and AFM analysis. The electrical stability and structural robustness of the matrix polymer is an important factor in obtaining operational reliability of composite type organic memory systems. This thermal robustness of the PI:PCBM system promises a stable functionality and long life time in organic memory device applications.

#### Acknowledgements

This study was achieved through support from the National Creative Research Laboratory Program (grant No. 2012026372) provided by the National Research Foundation of Korea (NRF), funded by the Korean Ministry of Science, ICT & Future Planning and the Research Institute of Advanced Materials (RIAM) of Seoul National University.

T.-W. Kim appreciates the financial support from the Korea Institute of Science and Technology (KIST) Institutional Program.

#### Appendix A. Supplementary data

Supplementary data related to this article can be found at <http://dx.doi.org/10.1016/j.orgel.2016.03.008>.

#### References

- [1] A.J. Heeger, S. Kivelson, J.R. Schrieffer, W.-P. Su, *Rev. Mod. Phys.* 60 (1988) 781.
- [2] G. Yu, J. Gao, J.C. Hummelen, F. Wudl, A.J. Heeger, *Science* 270 (1995) 1789.
- [3] S.R. Forrest, *Nature* 428 (2004) 911.
- [4] Y.-Y. Noh, N. Zhao, M. Caironi, H. Sirringhaus, *Nat. Nanotechnol.* 2 (2007) 784.
- [5] J. Rivnay, L.H. Jimison, J.E. Northrup, M.F. Toney, R. Noriega, S. Lu, T.J. Marks, A. Facchetti, A. Salleo, *Nat. Mater.* 8 (2009) 952.
- [6] H. Yan, Z. Chen, Y. Zheng, C. Newman, J.R. Quinn, F. Dötz, M. Kastler, A. Facchetti, *Nature* 457 (2009) 679.
- [7] T. Sekitani, H. Nakajima, H. Maeda, T. Fukushima, T. Aida, K. Hata, T. Someya, *Nat. Mater.* 8 (2009) 494.
- [8] L.D. Bozano, B.W. Kean, M. Beinhoff, K.R. Carter, P.M. Rice, J.C. Scott, *Adv. Funct. Mater.* 15 (2005) 1933.
- [9] Y. Ji, B. Cho, S. Song, T.-W. Kim, M. Choe, Y.H. Kahng, T. Lee, *Adv. Mater.* 22 (2010) 3071.
- [10] Y. Ji, D.F. Zeigler, D.S. Lee, H. Choi, A.K.-Y. Jen, H.C. Ko, T.-W. Kim, *Nat. Commun.* 4 (2013) 2707.
- [11] Q.-D. Ling, D.-J. Liaw, C. Zhu, D.S.-H. Chan, E.-T. Kang, K.-G. Neoh, *Prog. Polym. Sci.* 33 (2008) 917.
- [12] B. Cho, S. Song, Y. Ji, T.-W. Kim, T. Lee, *Adv. Funct. Mater.* 21 (2011) 2806.
- [13] J.C. Scott, L.D. Bozano, *Adv. Mater.* 19 (2007) 1452.
- [14] S.K. Hwang, J.M. Lee, S. Kim, J.S. Park, H.I. Park, C.W. Ahn, K.J. Lee, T. Lee, S.O. Kim, *Nano Lett.* 12 (2012) 2217.
- [15] Y. Song, H. Jeong, J. Jang, T.-Y. Kim, D. Yoo, Y. Kim, H. Jeong, T. Lee, *ACS Nano* 9 (2015) 7697.
- [16] J. Ouyang, C.-W. Chu, C.R. Szmamda, L. Ma, Y. Yang, *Nat. Mater.* 3 (2004) 918.
- [17] Y. Yang, J. Ouyang, L. Ma, R.J.-H. Tseng, C.-W. Chu, *Adv. Funct. Mater.* 16 (2006) 1001.
- [18] M. Guaita, *Br. Polym. J.* 18 (1986) 226.
- [19] M.M. Shapi, A. Hesso, *J. Anal. Appl. Pyrolysis* 18 (1990) 143.
- [20] L.E. Manring, D.Y. Sogah, G.M. Cohen, *Macromolecules* 22 (1989) 4652.
- [21] M.C. Costache, D. Wang, M.J. Heidecker, E. Manias, C.A. Wilkie, *Polym. Adv. Tech.* 17 (2006) 272.
- [22] J.A. Cella, *Polym. Degrad. Stabil.* 36 (1992) 99.
- [23] D.-J. Liaw, K.-L. Wang, Y.-C. Huang, K.-R. Lee, J.-Y. Lai, C.-S. Ha, *Prog. Polym. Sci.* 37 (2012) 907.
- [24] T.-W. Kim, H. Choi, S.-H. Oh, G. Wang, D.-Y. Kim, H. Hwang, T. Lee, *Adv. Mater.* 21 (2009) 2497.
- [25] B. Cho, T.-W. Kim, S. Song, Y. Ji, M. Jo, H. Hwang, G.-Y. Jung, T. Lee, *Adv. Mater.* 22 (2010) 1228.
- [26] S. Song, B. Cho, T.-W. Kim, Y. Ji, M. Jo, G. Wang, M. Choe, Y.H. Kahng, H. Hwang, T. Lee, *Adv. Mater.* 22 (2010) 5048.
- [27] Y. Song, J. Jang, D. Yoo, S.-H. Jung, S. Hong, J.-K. Lee, T. Lee, *Org. Electron.* 17 (2015) 192.
- [28] D. Yoo, Y. Song, J. Jang, W.-T. Hwang, S.-H. Jung, S. Hong, J.-K. Lee, T. Lee, *Org. Electron.* 21 (2015) 198.
- [29] S.H. Jo, K.-H. Kim, W. Lu, *Nano Lett.* 9 (2009) 496.
- [30] H.B. Lv, M. Yin, X.F. Fu, Y.L. Song, L. Tang, P. Zhou, C.H. Zhao, T.A. Tang, B.A. Chen, Y.Y. Lin, *IEEE Electron. Device Lett.* 29 (2008) 309.
- [31] J. Park, M. Jo, E.M. Bourim, J. Yoon, D.-J. Seong, J. Lee, W. Lee, H. Hwang, *IEEE Electron. Device Lett.* 31 (2010) 485.
- [32] C. Chen, C. Song, J. Yang, F. Zeng, F. Pan, *Appl. Phys. Lett.* 100 (2012) 253509.

- [33] F. Verbakel, S.C.J. Meskers, R.A.J. Janssen, H.L. Gomes, M. Cölle, M. Büchel, D.M. de Leeuw, *Appl. Phys. Lett.* 91 (2007) 192103.
- [34] B. Cho, S. Song, Y. Ji, T. Lee, *Appl. Phys. Lett.* 97 (2010) 063305.
- [35] B. Cho, J.-M. Yun, S. Song, Y. Ji, D.-Y. Kim, T. Lee, *Adv. Funct. Mater.* 21 (2011) 3976.
- [36] J.J. Kim, B. Cho, K.S. Kim, T. Lee, G.Y. Jung, *Adv. Mater.* 23 (2011) 2104.
- [37] T.-W. Kim, S.-H. Oh, J. Lee, H. Choi, G. Wang, J. Park, D.-Y. Kim, H. Hwang, T. Lee, *Org. Electron.* 11 (2010) 109.
- [38] M.A. Lampert, *Phys. Rev.* 103 (1956) 1648.
- [39] T.-W. Kim, S.-H. Oh, H. Choi, G. Wang, H. Hwang, D.-Y. Kim, T. Lee, *Appl. Phys. Lett.* 92 (2008) 253308.
- [40] J.-C. Chen, C.-L. Liu, Y.-S. Sun, S.-H. Tung, W.-C. Chen, *Soft Matter* 8 (2012) 526.
- [41] J.K. Baral, H.S. Majumdar, A. Laiho, H. Jiang, E.I. Kauppinen, R.H.A. Ras, J. Ruokolainen, O. Ikkala, R. Österbacka, *Nanotechnology* 19 (2008) 035203.